Khazar Journal of Water and Environment
DOI: 10.68277/kjwe.2026.14

e-ISSN: 3150-0188
khazarjournal.com

KJWE

# Geoelectrical Mapping and Environmental Assessment of Leachate-Induced Subsurface Contamination around an Open Dumpsite

**John Ejiofor Okonkwo[*a,b], Chidi Marcel Egeonu[b], Chinedu Ojo Igili[b],Joy Chiaka Ike[b],Onome Emmanuel Emudiaga[c],Merrious Oviri Ofomola[a]**

[a]*Department of Physics, Faculty of Science, Delta State University, Abraka Nigeria*
[b]*Department of Physical Sciences (Energy and Petroleum Studies), College of Natural & Applied Scences, Novena University, Ogume Nigeria*
[c]*Department of Applied Geophysics, Faculty of Science, Dennis Osadebay University, Asaba Nigeria*

ARTICLE INFO
Review Article
Corresponding Author: John Ejiofor Okonkwo, Email: jejiofor170@gmail.com
Received: 15 September 2026 / Revised: 26 October 2026 / Accepted: 10 November 2026 / Online: 15 November 2026

Cite this article as
Okonkwo, J. E., Egeonu, C. M., Igili, C. O., Ike, J. C., Emudiaga, O. E., & Ofomola, M. O. (2026). Geoelectrical Mapping and Environmental Assessment of Leachate-Induced Subsurface Contamination around an Open Dumpsite. Khazar Journal of Water and Environment, 1, 254–277. https://doi.org/10.68277/kjwe.2026.14.

## ABSTRACT

This study uses combined dipole–dipole and Schlumberger electrode arrays of electrical resistivity techniques to determine the amount of leachate migration and its possible effects on groundwater around an open dumpsite. The unfettered method of waste disposal in the area over time is concerning because it limits the potential sources of drinkable water for the expanding population. This influenced the environmental assessment of leachate migration to groundwater in the study area. Five vertical electrical sounding data were established along predefined traverses at accessible locations within the study area, despite field restrictions. 2D resistivity imaging profiles were conducted along these traverses to obtain detailed lateral and vertical subsurface resistivity variations. The results revealed four geoelectric layers which correspond to the topsoil, clay, sandy clay, clayey to fine medium grain sand and medium grain sand. The VES data revealed vertical variations in aquifer parameters, while 2-D profiles and geospatial maps showed their lateral and spatial distribution. Aquifer depth varies substantially: VES 3 is the main anomaly with the lowest resistivity (52.9 Ωm) and highest conductivity (~0.0189 S/m), likely the primary leachate zone. Protective capacity also varies, with longitudinal conductance highest at VES 3 (~0.1497 S) and lowest at VES 4 (~0.0101 S), while VES 1 (~0.0522 S), VES 2 (~0.0426 S), and VES 5 (~0.0387 S) are weak-to-poor, and the 2-D resistivity imaging profiles confirm conductive anomalies matching high-conductivity zones as probable migration paths versus resistive zones around VES 2 and VES 4 indicating weaker contamination evidence. Thus, this study shows the efficacy of electrical resistivity methods in mapping leachate generated from wastes in the dumpsite area. To avert groundwater contamination, restrict activities over weak protective areas, and use this study results to guide safe borehole placement and targeted monitoring.

**Keywords:** Leachate migration; Electrical resistivity; Groundwater contamination; Geoelectric profiling; Okpara dumpsite

## 1. Introduction

The increasing demand for ground water, coupled with environmental degradation and population growth, has necessitated the need for sustainable exploration, development, and management of aquifer systems (Okonkwo & Emmanuel, 2026; Harry *et al.,* 2018; Ezema *et al.,* 2020). The world's supply of clean fresh water is steadily decreasing because of disposing of urban waste materials, mainly domestic garbage, in land surface, shallow excavation, rivers and stream channels. These activities pose a serious threat of polluting both groundwater and downstream surface water. Pollution of groundwater happens mostly due to percolation of fluvial water and the infiltration of contaminants through the soil under waste disposal sites. These wastewaters become an integral part of soil–water hydrological system that humans depend on for survival. One of the most common demands in metropolitan areas includes detecting the location and extent of contamination patches in areas as small as landfills. In such circumstances, the integrated use of geophysical methods provides an important tool in the evaluation and characterization of contaminants generated by urban residues (domestic and/or industrial). Geo-electric, electromagnetic, magnetic and ground penetrating radar geophysical techniques can be applied in landfill investigations because dissolved plume (leachate) can influence resistivity/conductivity, dielectric constant, chargeability, and magnetic susceptibility. The electrical and electromagnetic (EM) methods are the most popular of the several non-invasive geophysical methods commonly used in sewage disposal site studies. Electrical and EM methods are able to detect changes related to variations in fluid content, chemical composition and temperature in the subsurface. Electrical resistivity is the physical property of rock and soil most affected by the presence of water. The electrical resistivity of rock and soil depends not only on the porosity of rocks and sediments at various depths, but also on their air and aqueous fluid content. Any variation in underground water chemistry may also affect their electrical properties (Mota *et al.,* 2004). The presence of contaminated fluids in the ground enhances electrical conductivity (EC). Electrical resistivity methods are essential tools in detailed mapping of contaminant plumes by measuring the resistivity distribution of the subsurface (Buselli *et al.,* 1992; Meju 2000). Continuous efforts toward providing high-quality water, while reducing water pollution using all means of resources have not yet yielded significant results (Alao, 2023; Alao, *et al.,* 2023). This study also applied a geophysical technique to identify an aquifer-promising zone with a very high overburden thickness overlaying the regional aquifer for effective groundwater development and sustainability. It engages on what is needed to be done to effectively manage water systems for local and national circumstances as well.

In the area, like in most other areas and cities, waste is generated daily and most of the wastes are discarded in improperly situated and dumping sites that are not engineered. Most of the dumping sites are located within residential areas, markets, farms, roadsides, and others. This threatens the groundwater and road facilities, not sparing the aesthetics of such affected areas. Unarguably, uncontrolled citing of boreholes as the source of potable water in most of our urban and rural communities as the government seemingly no longer provides the populace with water has become a serious challenge. However, maintaining a portable ground water supply that is free from microbial and chemical contaminants is far from reality in most of our urban centers, and in particular Okpara community, due to poor waste disposal and management practices. The challenge is worsened by the fact that there are inadequately trained waste disposal personnel and equipment, poor waste collection, sorting and disposal methods, and indiscriminate location of disposal sites without regards to the local geology and hydrogeology of the area (Olafisoye, 2013). All these contribute significantly to the contamination of soil and ground water. Recent industrial development and increased urbanization in the municipality have resulted in enormous generation of all kinds of waste ranging from municipal to industrial. The type of waste generated varies widely with many human activities located close to dumpsites. Industrial waste is generated from industrial activities such as chemicals, pesticides, paints, grease, inorganic materials, oil sludge, etc. while domestic wastes are those generated from commercial establishments and household activities. They occur in different forms, water – borne waste from households, including sewage, human and animal remains as well as chemical and laboratory waste. The release of these materials into the environment sometimes causes serious health problems. The level of wastes produced by dense human and domestic animal population often exceeds the local ecosystem's biodegradability, resulting in serious environmental pollution and epidemic outbreaks of diseases (Ronald, 1988). According to Parvin and Tareq, 2021, during the peak of the rainy season, the dumpsite is covered by flood water and this contributes to the formation of leachate. It is this contaminated liquid that enters into the soil and also eventually into the underlying groundwater at such dumpsites. A number of studies have been carried out to map possible areas for groundwater development that will be free from contaminants. Ehirim *et al.,* (2010) carried a geophysical and hydro-physiochemical study of the contaminant impact of a solid waste landfill (SWL) in Port Harcourt municipality, Nigeria and concluded that the contamination of ground water and soil is dominantly by landfill gases, while the excessive amount of micro-organisms is an indication of leachate contamination. Okunowo *et al.,* (2020) studied the application of the dipole–dipole and the Schlumberger electrode arrays of electrical resistivity techniques to map the extent of leachate migration and its possible impact on groundwater at Abule Egba, dumpsite, Lagos which revealed

that some regions around the dumpsite have been contaminated by leachate which could infiltrate to the unconfined aquifers in the area if not properly monitored and regulated. Thus, showing the efficacy of electrical resistivity method in mapping leachate generated from solid wastes in the dumpsite. The manner of disposal points to the fact that solid waste management is one of the greatest challenges facing state and local government environmental protection agencies in Nigeria. This work is aimed at investigating the effects of waste on groundwater by employing an integrated use of electrical resistivity arrays of Vertical electrical sounding with geospatial analysis to map the limit of the leachate contaminated zone.

## 2. Material and Methods

### *2.1. Study area*

Okpara Inland is a community located in the Ethiope East local government area of Delta State Nigeria (figure 1). Okpara Inland is bounded in the east by Kokori /Isiokolo, in the south by Ekrebuo/Orhoakpo, in the West by Ovu-inland. It is watered by Omue stream, which also runs across Kokori. Its thick forest had a substantial wildlife reserve, and its topography is very much okay for agricultural and pedestrian usage. The area lies between latitude N $05.532^0$ to N $05.822^0$ and longitude E $006.5996^0$ to E $006.015^0$ (figure 1), with an Elevation 23m to 36.2 m and Accuracy of 23.5 m to 55 m.

The hydrogeology of an area is controlled by factors such as geology as well as the climate of the region. This is true because the geological formations underlying the area and their structures determine the type of aquifers that would be developed and the means by which they would be recharged, and the climate determines the amount and rate of recharge of the aquifers (Olayinka, 2001; Zhody *et al.,* 1974). Okpara-Inland is underlain by the deposits of the Quaternary Sombreiro-Warri Deltaic Plain which consists of fine, medium and coarse grained, poorly sorted sands that occurs sometimes with occasional clay lenses, the thickness of these sands can be up to 30 m. The Sombreiro-Warri Deltaic Plain conformably overlies and masks the Benin Formation and is thought to be the recent expression of the Benin Formation (Aweto, 2012; Oomkens, 1974)

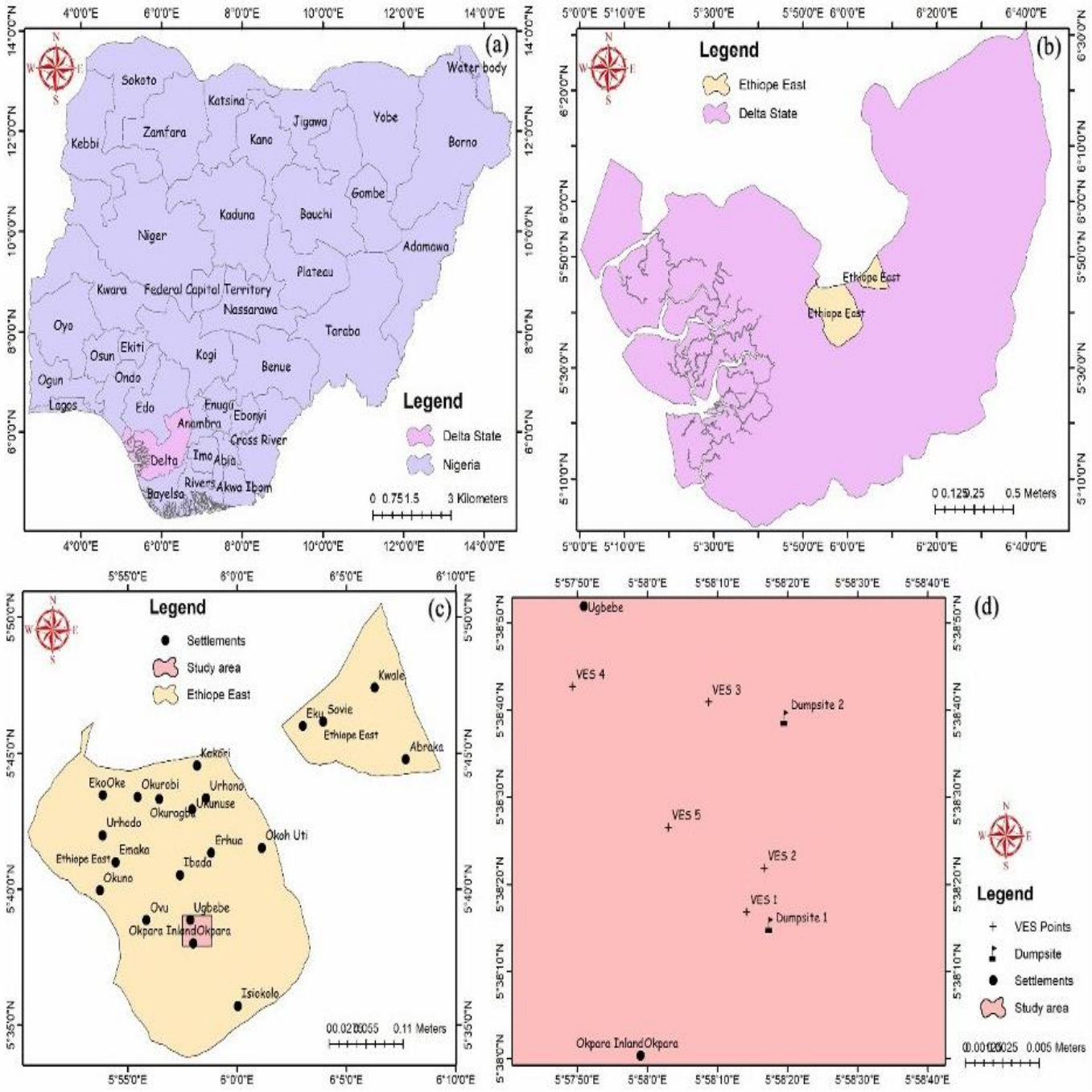



**Figure 1**. Location map showing (a) Nigeria with Delta State highlighted, (b) Delta State with Ethiope East area marked, (c) major settlements and road networks within Ethiope East LGA, and (d) layout of VES stations within the dumpsites survey area.

### *2.2. Data acquisition*

The electrical resistivity survey was carried out along two traverses with spread length of 150 m each using 2 Dipole-Dipole arrays and five schlumberger arrangement of vertical electrical soundings (VES). This was carried out to reveal the lateral and vertical variation of resistivity values beneath the dumpsite. The resistivity data was acquired using the ABEM 1000 Signal

Averaging System (SAS 1000) Terrameter. The other accessories were four (4) electrodes, measuring tape, four reels of cables, Garmin Global Positioning System (GPS). For the 2D resistivity measurements, the dipole–dipole array was deployed due to its greater depth of investigation, good horizontal resolution and data coverage (Koefoed, 1979). The data was acquired with minimum electrode spacing of 5 m and inter-electrode spacing ranging from 5 to 90 m. The spread of the traverses was based on the available space around the dumpsite. The co-ordinates of locations of measurements were recorded with GPS. The expansion factor (n) of the Dipole-dipole array varied from 1 to 5. The total length of each profile was 300 m. The dc-resistivity survey was conducted by introducing current into the subsurface with a current dipole (C1 and C2) and measuring the resulting ground voltage along the survey lines using the potential dipole (P1 and P2). Both pairs of electrodes (C1–C2 and P1--P2) are referred to as dipoles, and both dipoles have the same length (a). There is an increase in separation between the dipoles with each increase of depth.

In general, the apparent resistivity is given by;

$$\rho = 2\pi \frac{\Delta V}{I}\left[\frac{1}{r_1} - \frac{1}{r_2} - \frac{1}{r_3} - \frac{1}{r_4}\right] \quad (1)$$

Thus, the apparent resistivity for the dipole array is given as;

$$\rho = 2\pi \frac{\Delta V}{I}\left[\frac{1}{a+na} - \frac{1}{na} - \frac{1}{2a+na} + \frac{1}{a+na}\right] \quad (2)$$

$$\rho = 2\pi \frac{\Delta V}{I}\left[\frac{2}{(n+1)a} - \frac{1}{na} - \frac{1}{(n+2)a}\right]$$

$$\rho = 2\pi \frac{\Delta V}{I} \frac{n(n+1)(n+2)a}{2n^2+4n-(n^2+3n+2)-n^2+n}$$

$$\rho = \pi(n+1)(n+2)aR \quad (3)$$

Where $G = \pi a(n+1)(n+2)$

Therefore,

$$\rho = GxR \quad (4)$$

Equation (3) is the apparent resistivity for the Dipole – Dipole array. Where G is the geometric factor or the known value, a is the separation between current and potential electrodes and R the resistance.

### *2.3. Data processing*

WinRESIST version 1.0 for 1D inversion and curve matching, and DIPPRO 4.0 for 2D pseudosection generation were used to process the data. The software ran several iterations to minimize fitting errors. Pseudo-section profiles were compared against VES results and borehole lithology to check for consistency as quality control (QC) measures.

The 2D field resistivity data was obtained using the equation (3) above as;

$$\rho = \pi(n+1)(n+2)aR$$

where n = number of electrode spacing, a = electrode separation, V = resulting electric potential I = current injected.

After three iterations, the DIPRO 4.0 inversion software produced the inverted resistivity models. This was done to make sure the inversion models accurately depicted the geology of the research area and weren't smoothed out. Partial curve matching was used to quantitatively analyze the depth sounding curves for the VES data (Koefoed, 1979; Okunowo *et al*., 2020). Equation (4) was used to estimate the apparent resistivity values.

A resistivity and depth model was constructed from VES data using partial curve matching. The primary input for computer iteration in the WINRESIST 1.0 version software was the field-derived apparent resistivity data (Vander Velpen 1988). One-dimensional information about the earth was obtained from the final resistivity readings (Omosanya *et al*. 2014). Later, cross sections over the research area were interpolated using resistivity and thickness measurements and all five VES fit is reported as root mean square (RMS) misfit values = 4.3% (Figure. 3). The area's subsurface resistivity is contrasted with comparable resistivity readings from nearby borehole lithology obtained within the study area (Figure. 2). The electrical resistivity tomography (ERT) provides 2D information on subsurface resistivity and thickness. ERT is frequently used for detecting pollution (Chambers *et al*. 2006; Daily *et al*. 1998) and characterizing subsurface geologic unit (Daily *et al*. 1998; Goes and Meekes 2004). In addition, the profiling was used for validating the interpolated resistivity values from the electrical sounding (Omosanya *et al*. 2014). For the profiling, it was assumed that resistivity does not change in the direction that is perpendicular to the survey line. Dipole-dipole array configuration was used for the profiling with the survey line located on the dumpsite. The derived pseudosection were inverted, a process that allows the apparent resistivity to be plotted against the true depth rather than electrode spacing. The results obtained from the pseudosection was further interpreted by describing the resistivity of each layer as compared with the standard resistivity of rock types (Palacky 1988, Akinmosin *et al*. 2013). The protective

capacity of groundwater aquifers is a function of the covering layers usually referred to as the protective layers (Kirsch 2006). Surface water percolates through the protective layers leading to groundwater recharge. During this percolation process, contaminant degradation can occur by mechanical, physicochemical, and microbiological processes. An effective groundwater protection is given by protective layers with sufficient thickness and low hydraulic conductivity leading to high residence time of percolating water. (Mosuro *et al.,* 2017)

**Table 1.** Summary of results obtained from computer iteration

| VES | Layer | Resistivity (Ω·m) | Thickness (m) | Depth (m) | Curve type | Lithogy |
|---|---|---|---|---|---|---|
| 1 | 1 | 79.6 | 0.2 | 0.2 | QH | Topsoil |
| | 2 | 79.6 | 0.3 | 0.5 | | Clayed sand |
| | 3 | 79.3 | 3.64 | 4.14 | | Fine sand |
| | 4 | 261 | | | | Medium grain sand |
| 2 | 1 | 212 | 1.41 | 1.41 | HK | Topsoil |
| | 2 | 75.8 | 2.48 | 3.89 | | Clayed sand |
| | 3 | 1770 | 5.74 | 9.63 | | Fine sand |
| | 4 | 179 | | | | Medium grain sand |
| 3 | 1 | 87.9 | 1.67 | 1.67 | KH | Topsoil |
| | 2 | 1147 | 2.37 | 4.05 | | Clayed sand |
| | 3 | 52.9 | 7.71 | 11.8 | | Fine sand |
| | 4 | 35702 | | | | Medium grain sand |
| 4 | 1 | 336 | 0.5 | 0.5 | AK | Topsoil |
| | 2 | 496 | 3.88 | 4.38 | | Clayed sand |
| | 3 | 7336 | 5.58 | 9.96 | | Fine sand |
| | 4 | 527 | | | | Medium grain sand |
| 5 | 1 | 798 | 4.7 | 4.7 | KH | Topsoil |
| | 2 | 5215 | 5.15 | 9.85 | | Clayed sand |
| | 3 | 317 | 10.1 | 20 | | Fine sand |
| | 4 | 65808 | | | | Medium grain sand |

**Table 2.** Geoelectric Parameters for the study of aquifer Protective Capacity Rating

| VES | Layers | Resistivity $\rho$ (Ω.m) | Thickness (m) | Conductivity $\sigma = 1/\rho$ | $S = \sum_{i=1}^{n} \frac{h_i}{\rho_i}$ | Longitudinal Conductivity of protective layer | Protective Capacity rating | Protective Capacity rating |
|---|---|---|---|---|---|---|---|---|
| 1 | 1 | 79.6 | 0.2 | 0.2 | 0.012562814 | 0.00251256 | 0.01739435 | Weak |
| | 2 | 79.6 | 0.3 | 0.5 | 0.012562814 | 0.00376884 | | |
| | 3 | 79.3 | 3.64 | 4.14 | 0.01261034 | 0.04590164 | | |
| | 4 | 261 | | | 0.003831418 | | | |
| 2 | 1 | 212 | 1.41 | 1.41 | 0.004716981 | 0.00665094 | 0.01420385 | Weak |
| | 2 | 75.8 | 2.48 | 3.89 | 0.013192612 | 0.03271768 | | |
| | 3 | 1770 | 5.74 | 9.63 | 0.000564972 | 0.00324294 | | |
| | 4 | 179 | | | 0.005586592 | | | |
| 3 | 1 | 87.9 | 1.67 | 1.67 | 0.011376564 | 0.01899886 | 0.05560394 | Weak |
| | 2 | 1147 | 2.37 | 4.05 | 0.00087184 | 0.00206626 | | |
| | 3 | 52.9 | 7.71 | 11.8 | 0.018903592 | 0.14574669 | | |
| | 4 | 35702 | | | 0.000279486 | | | |
| 4 | 1 | 336 | 0.5 | 0.5 | 0.00297619 | 0.0014881 | 0.0033571 | Poor |
| | 2 | 496 | 3.88 | 4.38 | 0.002016129 | 0.00782258 | | |
| | 3 | 7336 | 5.58 | 9.96 | 0.000136314 | 0.00076063 | | |
| | 4 | 527 | | | 0.001897533 | | | |
| 5 | 1 | 798 | 4.7 | 4.7 | 0.001253133 | 0.00588972 | 0.01291282 | Poor |
| | 2 | 5215 | 5.15 | 9.85 | 0.000191755 | 0.00098754 | | |
| | 3 | 317 | 10.1 | 20 | 0.003154574 | 0.0318612 | | |
| | 4 | 65808 | | | 0.00015186 | | | |

## 3. Results and Discussions

### *3.1. 1D VES geo-resistivity sections*

The apparent resistivity values obtained were modelled and inverted to generate geoelectric parameters, which were then used to infer the nature and depth of underlying formations (Okonkwo

& Emmanuel, 2026). Table 1 shows the summary of results obtained from computer iteration of the study area. The high resistivity values obtained at the VES stations suggest that this part of the study area is not contaminated by the leachate. When contaminated by landfill leachate (which has a high ionic content), the resistivity of subsurface layers is significantly reduced, as leachate increases the electrical conductivity. Table 2: Geoelectric Parameters for the study of aquifer Protective Capacity Rating. Figure 5 shows the geoelectric section of the study area dumpsite revealing four (4) geo-electric layers; typical type KH curve was obtained. The first layer is the top soil of resistivity 79.6 ohm-m and 798 ohm-m, with thickness of 0.2 and 4.7 m. The second layer is underlain by clayed sand layer of 75.8 ohm-m and 5215 ohm- m with thickness of 0.3 m and 5.15 m. The third layer is fine to medium grain sand of resistivity 52.9 ohm-m and 7336 ohm-m with thickness 3.64 m and 10.1 m, respectively, the last layer is medium to coarse grain sand with resistivity values 179 ohm-m and 65808 ohm-m with an unknown thicknesses.

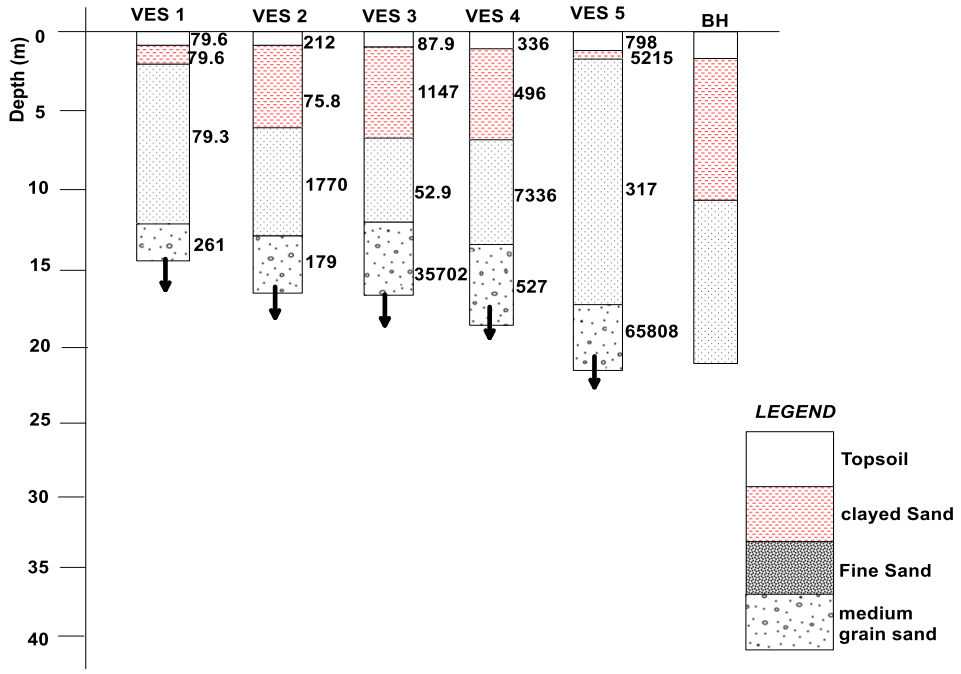
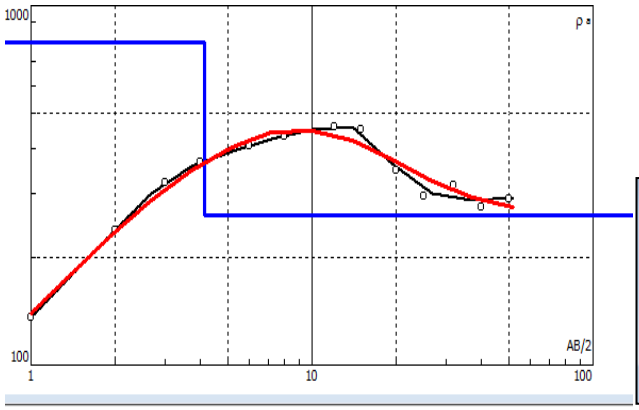



**Figure 2.** Geoelectric section of borehole lithology obtained within the study area

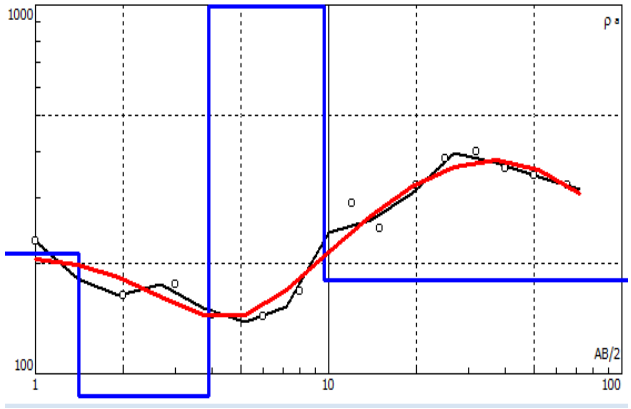
VES 1




RMS=4.3%

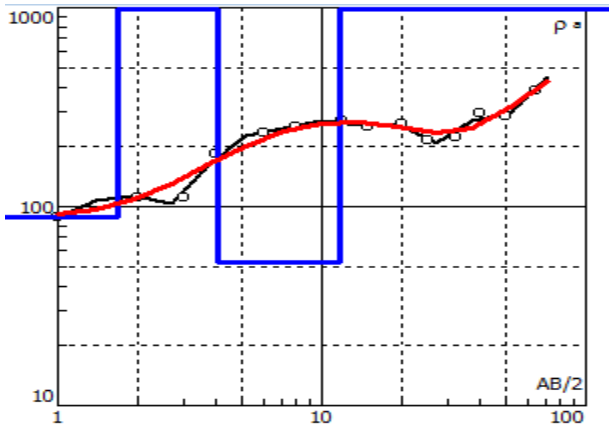
| N | ρ | h | d | Alt |
|---|---|---|---|---|
| 1 | 79.6 | 0.2 | 0.2 | -0.2 |
| 2 | 79.6 | 0.3 | 0.5 | -0.5 |
| 3 | 793 | 3.64 | 4.14 | -4.138 |
| 4 | 261 | | | |

VES 2



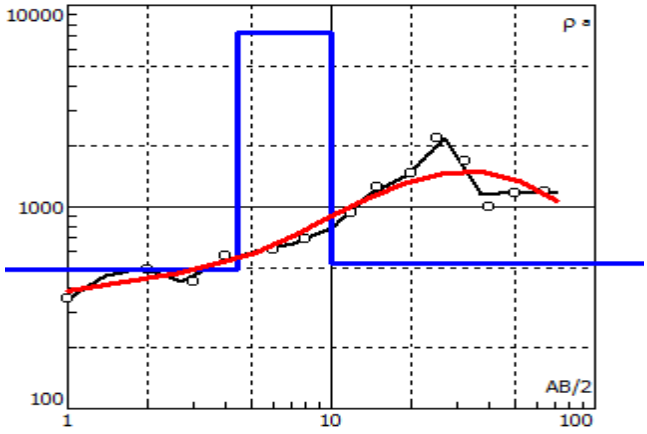

| N | ρ | h | d | Alt |
|---|---|---|---|---|
| 1 | 212 | 1.41 | 1.41 | -1.411 |
| 2 | 75.8 | 2.48 | 3.89 | -3.894 |
| 3 | 1770 | 5.74 | 9.63 | -9.631 |
| 4 | 179 | | | |

VES 3



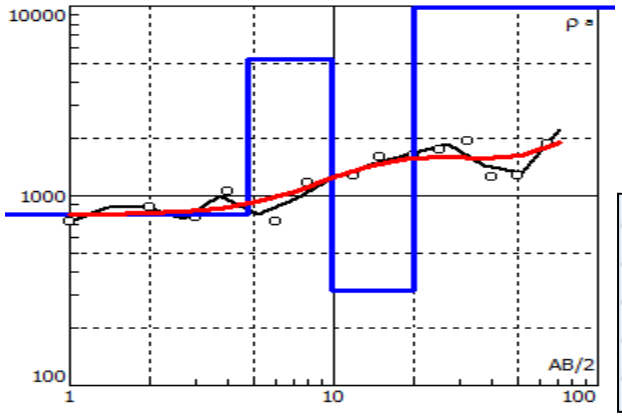

| N | ρ | h | d | Alt |
|---|---|---|---|---|
| 1 | 87.9 | 1.67 | 1.67 | -1.674 |
| 2 | 1147 | 2.37 | 4.05 | -4.048 |
| 3 | 52.9 | 7.71 | 11.8 | -11.75 |
| 4 | 35702 | | | |

VES 4




| N | ρ | h | d | Alt |
|---|---|---|---|---|
| 1 | 336 | 0.5 | 0.5 | -0.5 |
| 2 | 493 | 3.88 | 4.38 | -4.375 |
| 3 | 7336 | 5.58 | 9.96 | -9.955 |
| 4 | 527 | | | |

VES 5




| N | ρ | h | d | Alt |
|---|---|---|---|---|
| 1 | 798 | 4.7 | 4.7 | -4.7 |
| 2 | 5215 | 5.15 | 9.85 | -9.854 |
| 3 | 317 | 10.1 | 20 | -19.97 |
| 4 | 65808 | | | |

**Figure 3.** (VES 1 – 5) Plot for apparent resistivity against electrode spacing (AB/2) for the vertical electrical sounding inside the dumpsite

### *3.2. 2D electrical resistivity imaging results*

The 2-D resistivity profile was interpreted using the DIPRO software. The 2-D inverse models of the real electrical resistivity are displayed in Fig. 4a & 4b. They are used to display variation in subsurface resistivity with depth. Areas of extremely low resistivity values are attributed to leachate contamination and in the study are defined on 2-D inverse models as bowl-shaped anomalous zones interpreted as contamination plume (Mosuro *et al.,* 2017). The profile was done along the North-West direction through the dumpsite perpendicular to VES. The pseudosection revealed low resistivity value of (5.7 – 49 ohm-m) attributed to the presence of highly conductive leachate which indicates that the area has been contaminated. The blue section shows zone of low resistivity (contaminant leachate plume), the green portion in the southern portion from the surface to depth of 2.5 m is composed of a sandy clay/top soil which presumably inhibit the percolation of leachate. Consequently, two zones were observed on the profile; they are the zones of high and low

resistivity as shown in figure 4a & 4b. Contaminant leachate plume was identified in 2-D resistivity profile as the section of low resistivity zone represented by blue contour. The observed contamination is consistent with the earlier work (Ehirim *et al*., 2009; Esmail *et al*., 2008; Samsudeen *et al*., 2006; Olayinka and Olayiwola, 2001).

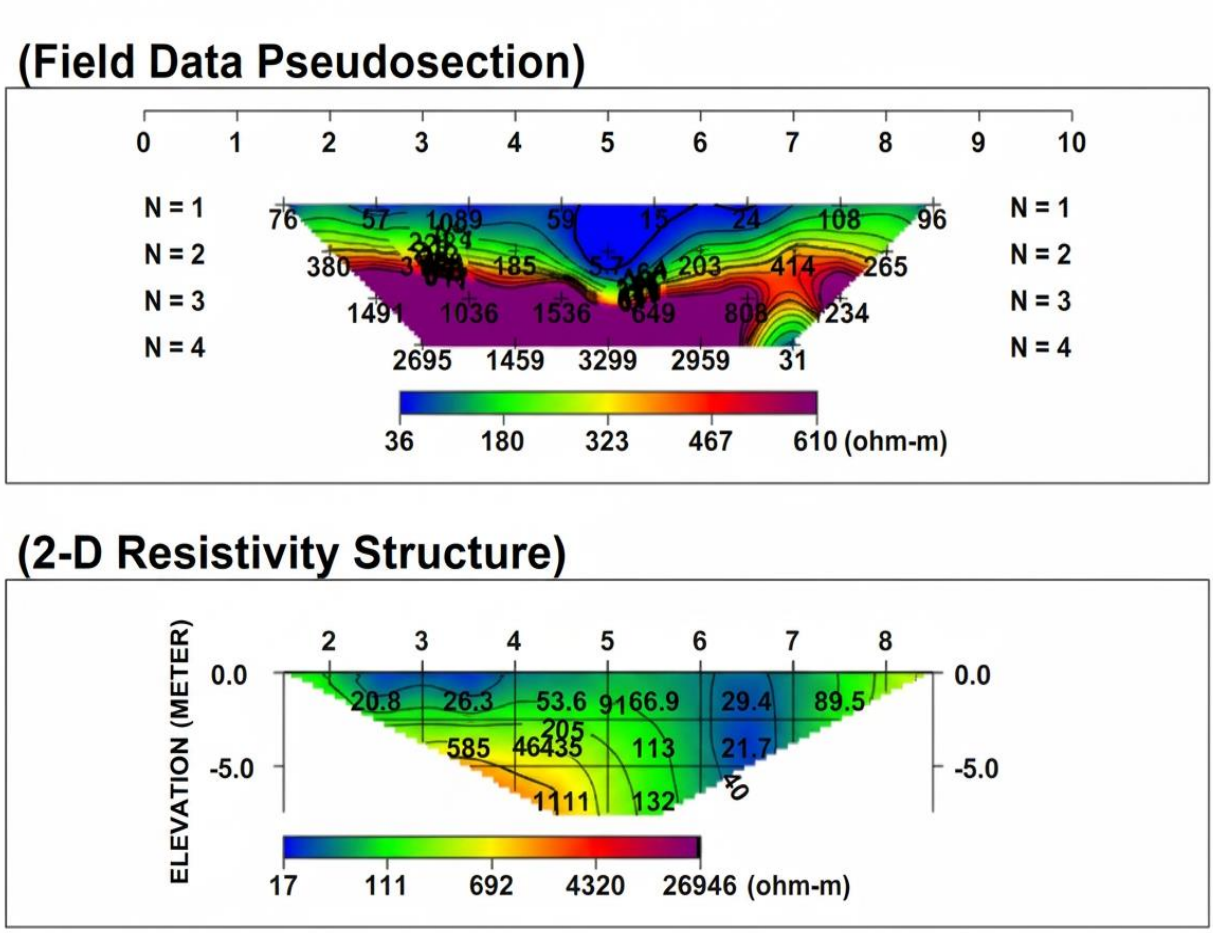



**Figure 4a.** Resistivity pseudo section for profiles 1. The resistivity values are contoured using different colors

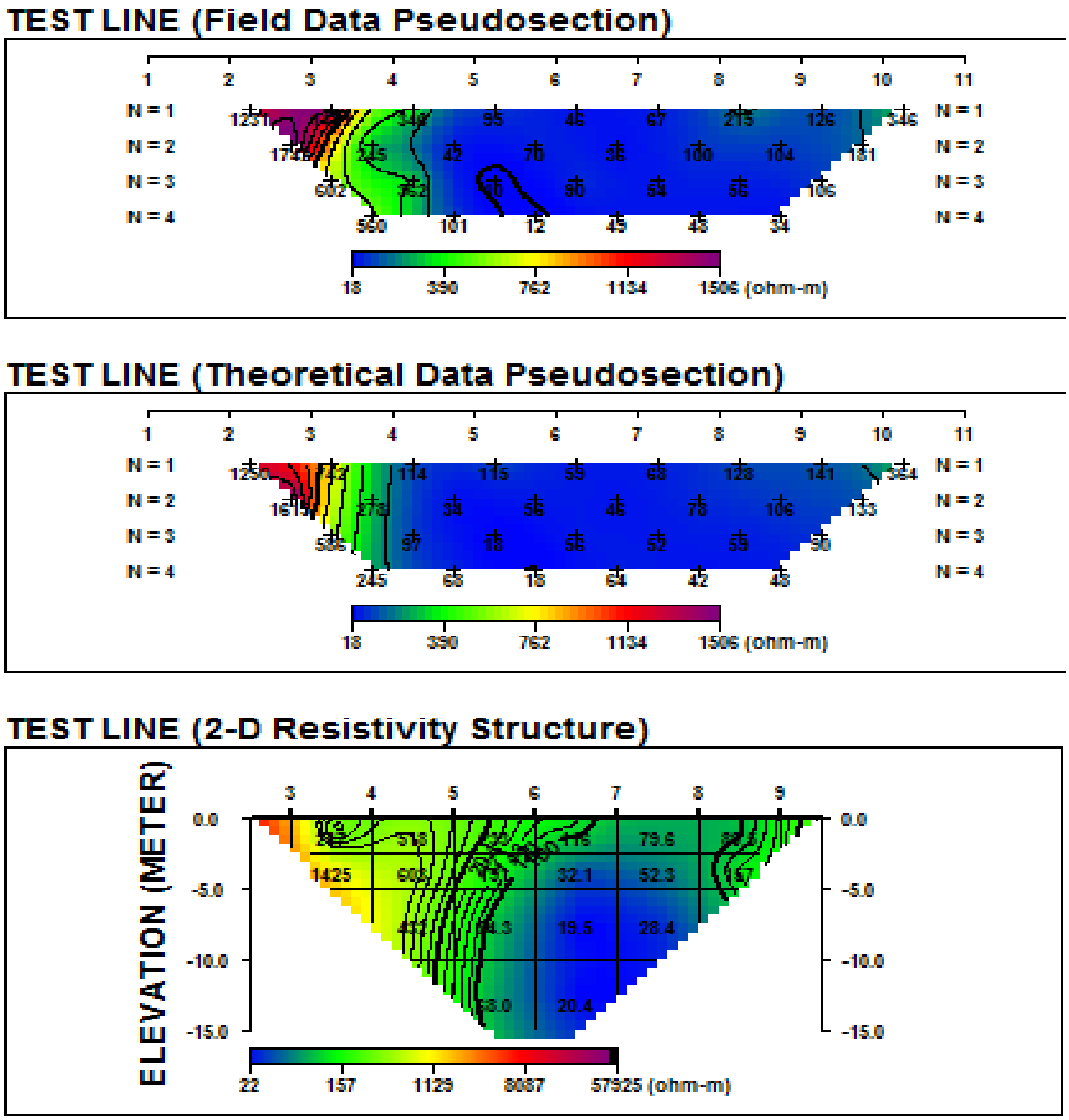



**Figure 4b.** Resistivity pseudo section for profiles 2. The resistivity values are contoured using different colors

### *3.3. Spatial distribution and hydrogeological implications of aquifer parameters*

The geographic variation in aquifer resistivity, thickness, and conductivity offers important information on Okpara inland community subsurface hydrogeology and groundwater development

suitability. The results of these parameters, which were obtained from five VES sites, are discussed in this section along with their implications for ground water potential and aquifer characteristics.

The area studied exhibits significant variation in the geographical distribution of aquifer resistivity, as seen in figure. 5. The range of resistivity values, which show variations in water saturation levels and lithological composition, is 53 Ω.m to 7336 Ω.m. The existence of dry or well-consolidated coarse sands and medium grain, which are typical of productive aquifers with low clay content and high permeability, is suggested by the greatest resistivity values found at VES 4 (7336 Ω.m) and VES 5 (65808 Ω.m). On the other hand, VES 1 (79.3 Ω.m), VES 2 (75.8 Ω.m), and VES 3 (52.9 Ω.m) have the lowest resistivity values, suggesting highly saturated or clay-rich formations. These formations are usually associated with leachate pollution zones and have high ion content. Resistivity tends to increase in the western and northwestern parts (e.g., VES 5 and VES 4) and decrease in the central and central-eastern portion of the research area (about VES 1; VES 3 and VES 2). Variations in aquifer saturation levels and lithologic transitions are reflected in this pattern.

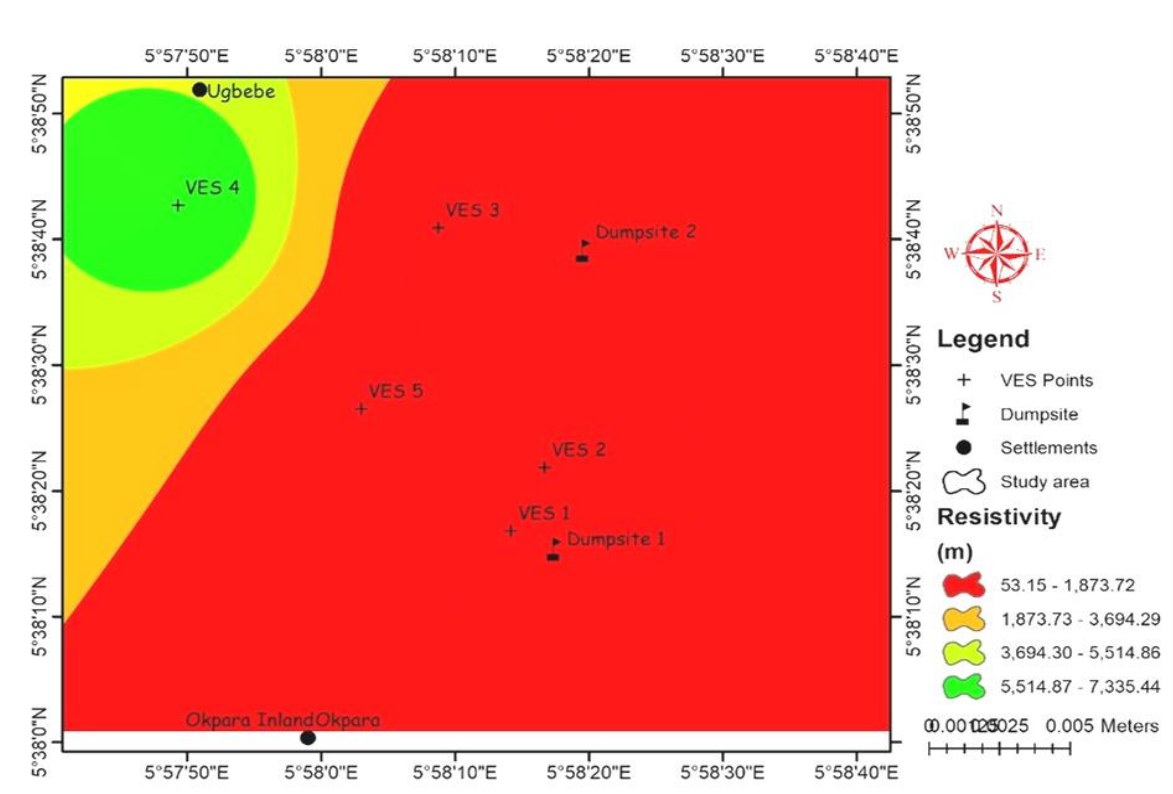



**Figure 5.** Spatial distribution of aquifer resistivity in the study area

Aquifer thickness varies considerably across the study area (Okonkwo *et al.,* 2025) , as shown in figure 6, ranging from 0.2 m at VES 1—10.1 m at VES 5. The thickest aquifers are concentrated in the central zone (VES 5), where fine to medium grained sands were identified in the geoelectric

models. These areas indicating relatively thick and potentially productive aquiferous horizon with considerable vulnerability to leachate-induced contamination. Its permeable nature may facilitate the downward migration and lateral dispersion of dissolved contaminants from the dumpsite into the groundwater system. Although the relatively high resistivity value in the layer of value 317 Ω.m does not provide strong evidence of significant present contaminant at the VES station, the considerable thickness of the aquifer implies a substantial contaminant transport and storage potential if leachate gains hydraulic access to the unit. Consequently, VES 5 should be regarded as potentially vulnerable groundwater zone requiring monitoring, particularly in the direction of groundwater flow from the dumpsite. Moderate aquifer thicknesses, ranging from 3.64 to 7.71 m, are found around VES 1, VES 2 and VES 4, indicating a moderate capacity of contaminant migration and storage, implying that these locatioins may be vulnerable to leachate induced groundwater contamination where hydraulic connectivity with the dumpsite exists, however suggests a reduced contaminant transport and storage capacity. The overlying clayed-sand layer may further provide potential protection by retarding the downward migration of leachate. From a spatial standpoint, aquifer thickness is most significant in the central part of the study area, decreasing toward the northwest and southeastern margins. This trend may be influenced by subsurface structural variations or paleochannel formations that concentrate fluvial sand deposits in certain zones (Okonkwo & Emmanuel, 2026; Adewumi *et al.,* 2023).

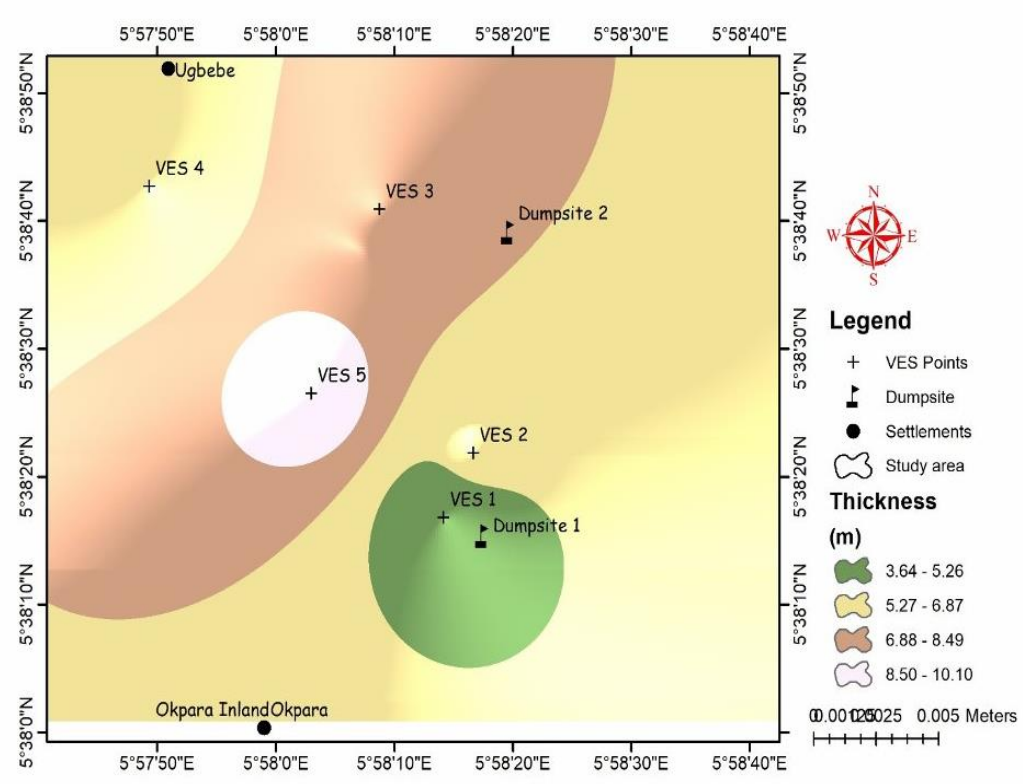



**Figure 6.** Spatial distribution of aquifer thickness in the study area

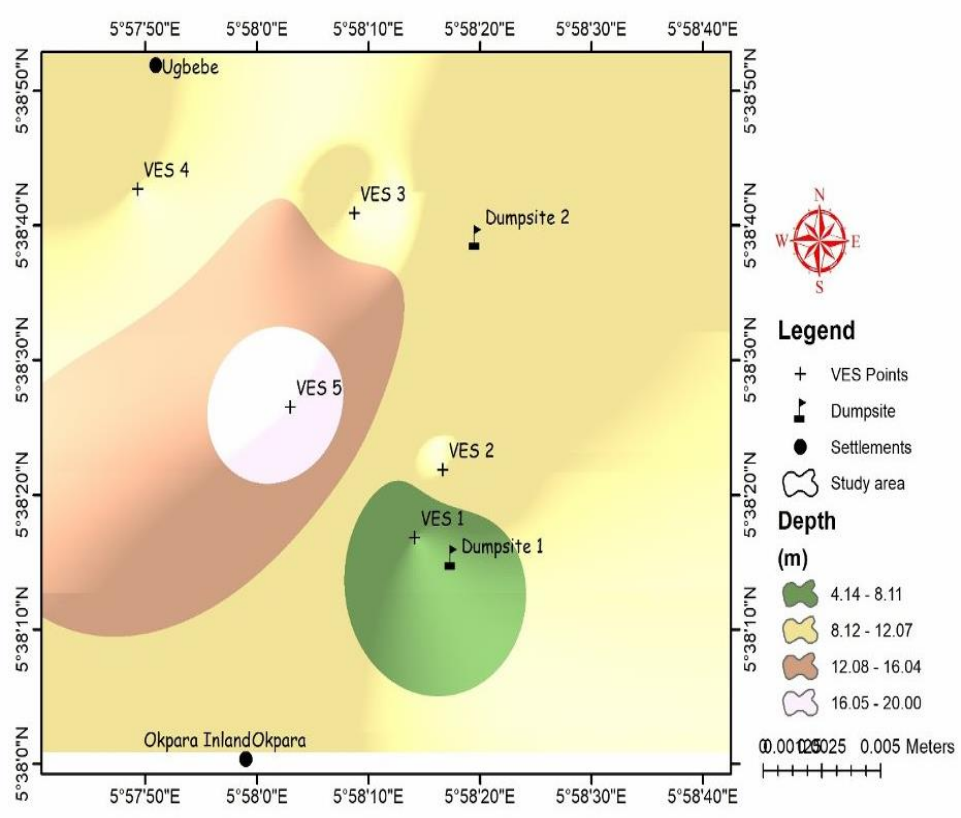



**Figure 7.** Spatial distribution of aquifer depth in the study area

The depth distribution of the interpreted aquiferous units reveals considerable vertical and lateral variation across the study area, with the top of the principal fine-sand aquifer occurring at approximately 0.50 m at VES 1 and progressively deeper at VES 2 (3.89 m), VES 3 (4.05 m), VES 4 (4.38 m) and VES 5 (9.85 m). The shallow occurrence of the aquifer at VES 1 implies high susceptibility to direct leachate infiltration, whereas the greater depth at VES 5 provides comparatively greater protection and opportunity for natural attenuation. Nevertheless, the substantial 10.1 m thickness of the VES 5 aquifer means that, once reached, contaminants could be transported and stored within a considerable permeable interval. VES 3 is particularly significant because its aquifer occurs at a moderate depth and exhibits an anomalously low resistivity of 52.9 Ωm, suggesting possible leachate influence. Overall, as seen in figure 7, the depth variations indicate spatially heterogeneous groundwater vulnerability and leachate migration potential across the study area.

The calculated aquifer conductivity reveals considerable spatial variation in the electrical properties of the groundwater-bearing formations. The ionic content of groundwater, porosity, and permeability all have a significant impact on aquifer conductivity, which corresponds inversely with resistivity. The fine-sand aquifer at VES 3 exhibits the highest conductivity of approximately 0.0189 S/m, corresponding to a low resistivity of 52.9 Ωm, followed by VES 1 (0.0126 S/m) and

VES 5 (0.00315 S/m). The relatively elevated conductivity at VES 3 may reflect increased ionic concentration within the pore water and is potentially associated with leachate infiltration from the dumpsite. This interpretation is further supported by the considerable thickness of the fine-sand unit (7.71 m), its occurrence at moderate depth and its weak protective capacity. Conversely, the low conductivity values recorded at VES 2 (0.000565 S/m) and VES 4 (0.000136 S/m) indicate comparatively resistive aquifer conditions with less evidence of conductive contaminant loading. The moderate conductivity at VES 5, despite its relatively thick 10.1 m aquifer, indicates the need for continued monitoring because of its substantial potential for contaminant transport and storage. Overall, the conductivity distribution suggests that VES 3 represents the most probable zone of leachate-induced groundwater quality deterioration, while VES 1 and VES 5 constitute additional zones of concern. As seen in figure. 8, the north-central zones exhibit relatively high conductivity values, while the south-central display lower values.

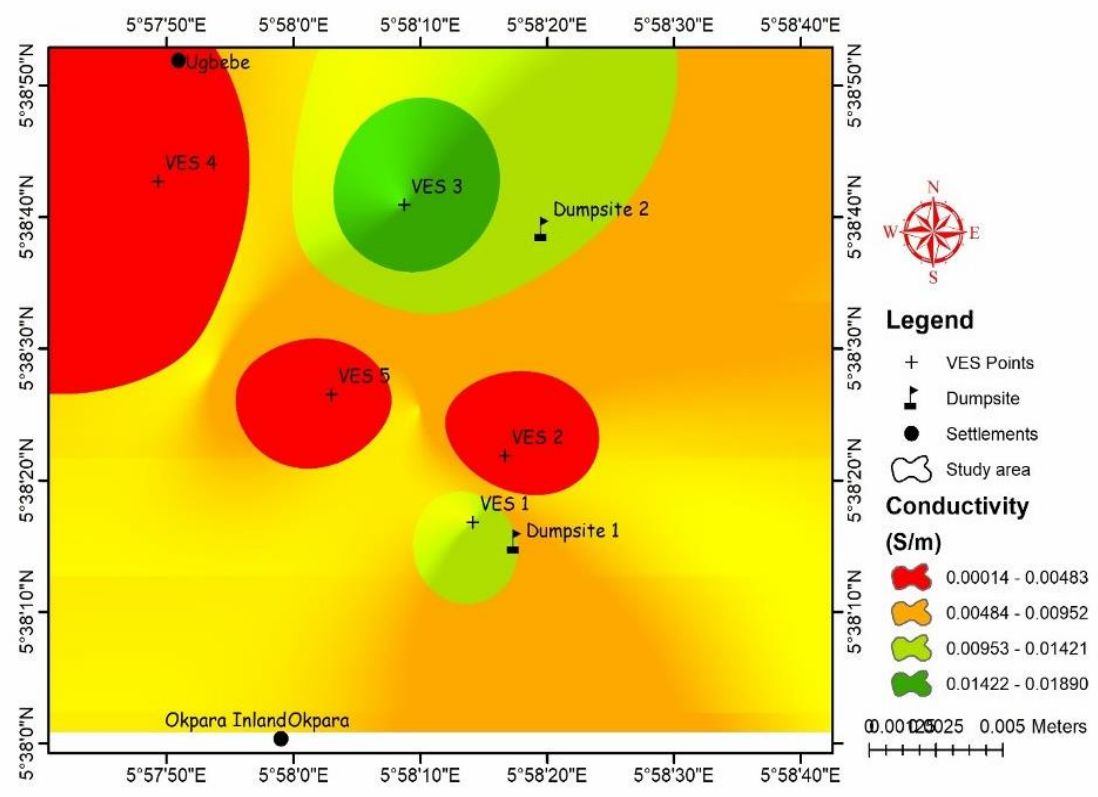



**Figure 8.** Spatial distribution of aquifer conductivity (S/m) in the study area

Longitudinal conductance (S), determined by the quotient of layer thickness and resistivity, acts as a measure of the protective capacity of overburden layers against surface contaminants. Higher values suggest better shielding due to the presence of conductive materials such as clay or silty clay, which hinder pollutant migration (Okonkwo & Emmanuel, 2026; Bayewu *et al.,* 2018). As shown in

figure. 9. The calculated longitudinal conductance values range from 0.0101 to 0.1497 S across the investigated VES stations. VES 3 records the highest longitudinal conductance (0.1497 S), indicating comparatively greater protective capacity and potentially higher ability of the overlying materials to retard downward migration of leachate. Simultaneously, as earlier reported in Table 1 and 2. VES 3 also shows the lowest resistivity (52.9 Ωm) and highest conductivity (~0.0189 S/m) in a fine sand aquifer, interpreted as the principal probable leachate-affected zone. Therefore, this indicates that the high conductance at VES 3 may not reflect effective protection, but rather the impact of contaminant infiltration. hence, care must be taken in such settings not to rely solely on conductance for vulnerability assessment, but to integrate all geophysical indicators and contaminant evidence. VES 4 exhibits the lowest value (0.0101 S), signifying poor protective capacity. VES 1 and VES 2, with conductance values of 0.0522 and 0.0426 S, respectively, indicate weak protective conditions, while VES 5 records a low conductance value of 0.0387 S despite having the thickest fine-sand aquifer (10.1 m). The generally low longitudinal conductance values suggest that the overlying formations provide limited protection against downward migration of contaminants. Consequently, the aquifer systems, particularly around VES 4 and VES 5, may be susceptible to leachate-induced contamination where hydraulic connectivity exists. The low resistivity and high conductivity observed at VES 3 further suggest that leachate influence may already be present despite its relatively higher longitudinal conductance.

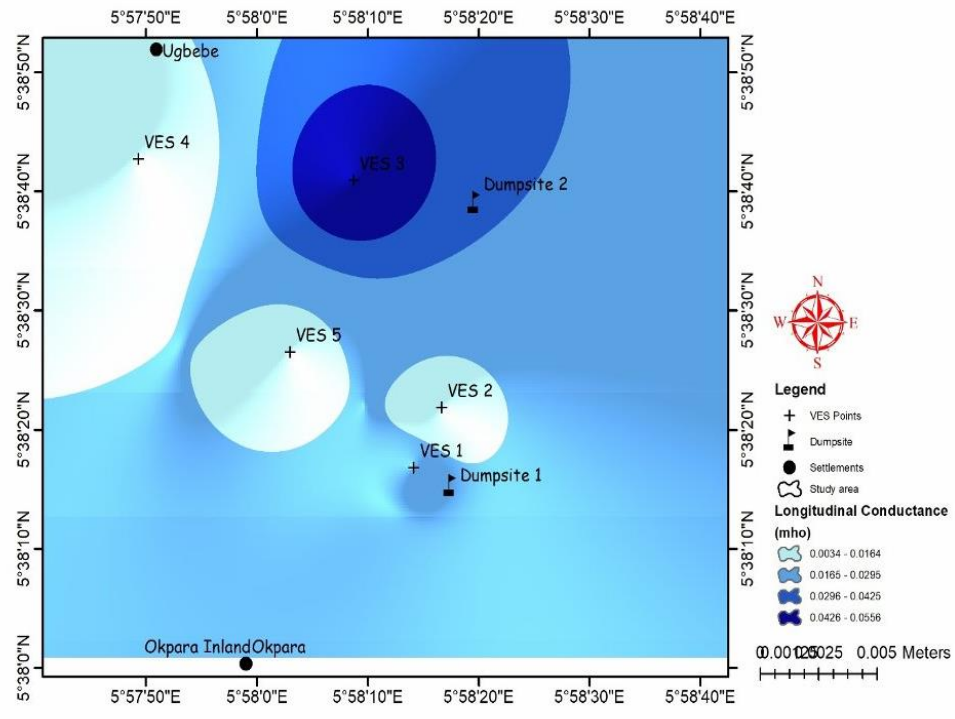



**Figure 9.** Spatial distribution of longitudinal conductance across the study area

## 4. Conclusions

The integration of Vertical Electrical Sounding (VES), the 2-D resistivity imaging, and GIS maps provide a comprehensive assessment of the subsurface conditions and potential leachate-induced contamination around the study area. The VES data established the vertical variation in lithology, aquifer depth and thickness, resistivity, conductivity, and longitudinal conductance, while the two Dipole–Dipole electrical resistivity profiles provided 2-D visualization of the lateral and vertical continuity of resistivity anomalies. The geospatial maps further demonstrated how these parameters are spatially distributed across the area. The aquifer-depth distribution map indicates substantial spatial variability in the depth to the principal aquifer. The shallow aquifer around VES 1 represents a highly vulnerable zone because the limited thickness of the overlying materials provides a shorter pathway for surface-derived leachate to reach groundwater. In contrast, the deeper aquifer around VES 5 provides greater separation from the surface but, because of its considerable thickness (~10.1 m), may serve as an important medium for contaminant storage and migration if and when contaminants eventually reach that depth. The aquifer-resistivity and conductivity distribution maps provide important evidence for identifying potential contamination zones. VES 3, characterized by the lowest aquifer resistivity (52.9 Ωm) and highest conductivity (~0.0189 S/m), constitutes the most prominent geoelectrical anomaly in the study area. If this location coincides spatially with the low-resistivity zones identified on the two electrical resistivity imaging profiles, the combined evidence strongly supports its interpretation as the principal probable leachate-affected zone. The longitudinal conductance/protective-capacity map further reveals considerable heterogeneity in the natural protection offered by the overburden. VES 3 has the highest longitudinal conductance (~0.1497 S), which when coincide with its reported low resistivity anomaly indicate possible impact of contaminant infiltration, whereas VES 4 has the lowest (~0.0101 S), indicating poor protection. VES 1, VES 2, and VES 5 have values of approximately 0.0522, 0.0426, and 0.0387 S, respectively, representing generally weak-to-poor protective conditions. The Dipole–Dipole 2-D profiles provide spatial confirmation of these point-based VES interpretations by imaging conductive and resistive zones between measurement locations. Conductive 2-D resistivity imaging anomalies that spatially correspond with the high-conductivity zones on the GIS maps provide stronger evidence for possible leachate migration. Conversely, resistive zones corresponding to the higher-resistivity areas mapped around VES 2 and VES 4 indicate comparatively weaker geoelectrical evidence of present contamination.

Notwithstanding the findings of this study, certain methodological limitations should be acknowledged when interpreting the reults. Electrical resistivity array techniques are used to detect subsurface conductive anomalies. However, the low resistivity zones cannot be solely attributed to

leachate pollution. Similar reactions may be caused by naturally occurring clay-rich lithologies, variations in moisture content and high pore-water ionic concentrations. Accordingly, the anomalies identified in this study were regarded as possible markers of leachate-affected areas, and not as definite proof of contamination. The advantages of the combined use of electrical resistivity imaging and hydrochemical investigations for better identification and assessment of landfill leachate contaminants have been shown in previous studies (Igboama et al., 2022; Alao et al., 2024). Thus, future research in the area should include the complement of geological studies, geophysical surveys and laboratory analyzes of soil and groundwater samples for relevant hydrochemical parameters (pH, electrical conductivity, total dissolved solids, major ions and potentially toxic elements) should be made in an effort to evaluate the contamination on its own, and to separate the effects of leachate from those of the natural geological variability. Also, the field conditions imposed restrictions on the availability of suitable locations for the establishment of the electrode arrays necessary in the study area. We remained steadfast in our dedication to surveying the area and collected VES data at the accessible and appropriate locations along the designated traverses, despite the challenge. Consequently, the VES results were employed as targeted supporting information, which was further enhanced by the 2-D resistivity imaging and GIS integration, rather than as comprehensive coverage of every location. Furthermore, in the lack of direct hydrogeological (pumping test or piezometric) data, comprehensive hydrogeological assessment including hydraulic conductivity or gradient information cannot be established. However, where these direct hydraulic parameters are unavailable, thicker aquifer units especially permeable fine sands and medium grain are typically interpreted as having a greater capacity to store and potentially allow the movement of contaminants. Thus**,** results regarding transport and storage potential are inferred predominantly from geoelectric/aquifer thickness correlations as in this study.

## Acknowledgements

The authors would like to thank all those who assisted in conducting this work. Artificial intelligence (AI) assisted tools were used only for grammatical corrections. No other AI was used to prepare this manuscript. The authors assume full responsibility for the manuscript's content, accuracy, and integrity.

## Author Declarations

**Authors' contributions:** Writing – review & editing, Writing – original draft, Visualization, Validation, Software, Methodology, Investigation, Formal analysis, Conceptualization, Data curation: J. E. O, Writing – review & editing, Writing – original draft, Supervision, Resources,

Project administration: C. M. E, Writing – original draft, Supervision, Resources: C. O. I, Conceptualization, Methodology, Investigation: J. C. I. Validation, Software, Methodology, Investigation, Formal analysis, Conceptualization: O. E. E, Writing – review & editing: M. O. O. All authors reviewed the manuscript

**Conflict of interest/Competing interests:** The authors declare no conflict of interest.

**Ethics approval/declarations:** No need/ Not applicable.

**Funding:** This research received no external funding.

**Consent to participate:** No need/ Not applicable.

**Consent for publication:** No need/ Not applicable.

**Data availability**: Data are available on request due to privacy or other restrictions.

## References

Adewumi, R, Agbasi, O. E., & Mayowa, A. (2023). Investigating ground water potential in northeastern basement complexes: a Pulka case study using geospatial and geo-electrical techniques. *HydroRes*;6:73—88. https://doi.org/10.1016/ j.hydres.2023.02.003.

Akinmosin, A.A., Omosanya, K.O., & Ige, T, (2013), The occurrence of Bitumen in Ijebu-itele, Eastern Dahomey Basin, SW, Nigeria. *ARPN J Sci Technol* 3(1):98–105

Alao, J. O. (2023). Impacts of Open Dumpsite Leachates on Soil and Groundwater Quality. *Groundwater for Sustainable Development, 20,* Article ID: 100877.https://doi.org/10.1016/j.gsd.2022.100877

Alao, J. O., Fahad, A., Abdo, H. G., Ayejoto, D. A., Almohamad, H., Ahmad, M. S., Nur, M. S., Danjuma, T. T., Yusuf, M. A., Francis, O. T., & Joy, A. O. (2023). RETRACTED: Effects of dumpsite leachate plumes on surface and groundwater and the possible public health risks.*The Science of the Total Environment*, *897*, 165469. *https://doi.org/10.1016/j.scitotenv.2023.165469*

Alao, J. O., Otorkpa, O. J., Abubakar, F., Eshimiakhe, D., Aliyu, A., Abdulsalami, M., & Abdulmalik, D. O. (2024). Geoelectrical resistivity and geochemistry monitoring of landfill leachates due to the seasonal variations and the implications on groundwater systems and public health. *Scientific Reports*, *14*(1), 26542. https://doi.org/10.1038/s41598-024-77727-6

Aweto, K.E. (2012). Hydrogeological Deductions from Geoelectric and Downhole Geophysical Data in Okpara Inland, Western Niger Delta, Nigeria. *Middle-East Journal of Scientific Research* 11 (1): 100-105, 2012

Bayewu, O.O, Oloruntola, M.O., Mosuro ,G.O., Laniyan, T.A., Ariyo, S.O., & Fatoba, J.O. (2018). Assessment of groundwater prospect and aquifer protective capacity using resistivity method in Olabisi Onabanjo University campus, Ago-Iwoye, South western Nigeria. *NRIAG J Astron Geophys*;7(2): 347—60. https://doi.org/10.1016/j.nrjag.2018.05.002.

Buselli, G., Davis, G.B., Barber, C., Height, M.I., & Howard, S.H.D. (1992). The application of electromagnetic and electrical methods to groundwater pollution problems in urban environments. *Explor Geophys* 23:543–556

Chambers, J.E., Kuras, O., Meldrum, P.I., Ogilvy, R.D, & Hollands, J. (2006). Electrical resistivity tomography applied to geologic, hydroge ologic, and engineering investigations at a former waste-disposal site. *Geophysics* 71(6):231–239

Daily, W. Ramirez, A., & Johnson, R. (1998). Electrical impedance tomography of a perchloroethelyne release. *J Environ Eng Geophys* 2:189–201

DIPRO TM Version 4.01 (2001) Processing and interpretation software for electri cal resistivity data. Korea Institute of Geoscience and Mineral Resources (KIGAM), Daejeon, South Korea

Ehirim, C.N., & Nwankwo, C.N. (2010) Evaluation of Aquifer Characteristics and Groundwater Quality using Geoelectric Method in Choba, Port Harcourt. *Archives of Applied Sciences in Research*, 2, 396-403.

Ehirim,C.N., Ebeniro, J.O., & Olanegan O.P. (2009). "A Geophysical Investigation of Solid Waste Landfill Using 2-D Resistivity Imaging and Vertical Electrical Sounding Methods in Port Harcourt Municipality, Rivers State, Nigeria" *Pacific J. Sci. Technol*. 10(2):Pp604-613.

Esmail, A.L, Abahi, A., Samsudeen, W., Uwari, W., Accob, Y.,& Umar, H. (2008). "2 -D Electrical Resistivity Investigation at Ampar Ten Ang Landfill Site, *Selangor D.E*.".Pp.342-367.

Ezema, O.K., Ibuot, J.C., & Obiora, D.N. (2020). Geophysical investigation of aquifer repositories in Ibagwa Aka, Enugu State, Nigeria, using electrical resistivity method. *Groundwater Sustain Dev* ;11:100458. https://doi.org/10.1016/j.gsd.2020.

Goes, B.J. M., & Meekes, J.A.C. (2004). An effective electrode configuration for the detection of DNAPLs with electrical resistivity tomog raphy. *J Environ Eng Geopys* 9:127–141

Harry, T.A., Ushie, F.A., & Agbasi, O.E. (2018). Hydraulic and geoelectric relationships of aquifers using vertical electrical sounding (VES) in parts of Obudu, Southern Nigeria. *World Sci News* ;94(2):261—75.

Igboama, W. N., Hammed, O. S., Fatoba, J. O., Aroyehun, M. T., & Ehiabhili, J. C. (2022). Review article on impact of groundwater contamination due to dumpsites using geophysical and physiochemical methods. *Applied Water Science*, *12*(6). https://doi.org/10.1007/s13201-022-01653-z

Kirsch, R. (2006) Groundwater protection: vulnerability of aquifers. In: Kirsh R (ed) Groundwater geophysics a tool for hydrogeology. *Springer, Berlin, Heidelberg*, pp 468–480

Koefoed, O. (1979). Geosounding principle, resistivity sounding measurements. *Elsevier Scientific Publishing, Amsterdam*

Meju, M.A. (2000). Geoelectrical investiga tion of old abandoned, covered landfill sites in urban areas: model development with a genetic diagnosis approach. *J Appl Geophys* 44:115–150

Mosuro, G.O., Omosanya, K.O., Bayewu, O.O., Oloruntola, M.O., Laniyan, T.A., Atobi, O., Okubena, M., Popoola, E.A., & Adekoya, F. (2017). Assessment of groundwater vulnerability to leachate infiltration using electrical resistivity method. *Applied Water Science, 7*, 2195-2207.

Mota, R., Monteiro-Santos, F.A., Mateus, A., Marques, F.O., Goncalves, M.A., &Figueiras Amaral. J.H. (2004). Granite frac turing and incipient pollution beneath a recent landfill facility as detected by geoelectrical surveys. *J Appl Geophys* 57:11–22

Okonkwo, J.E., & Emmanuel, E.D. (2026). "Appraisal of aquifer protective capacity and groundwater potential using the vertical electrical sounding technique in Illah, Delta State, Nigeria," *Al-Bahir*: Vol. 8: Iss. 1, Article 9.https://doi.org/10.55810/2313-0083.1118

Okonkwo, J.E., Agbasi, O.E.,& Igili, C.O. (2025). Evaluating the spatial influence of topography and land use on aquifer transmissivity in sedimentary terrains of Delta State, Nigeria. *Int J Energ Water Res* **9**, 2061–2077https://doi.org/10.1007/s42108-025-00375-7

Okunowo, O.O., Adeogun, O.Y., Ishola, K.S., &Alli, S. (2020): Delineation of leachate at a dumpsite using geo-electrical resistivity method: a case study of Abule Egba,Lagos, Nigeria. *SN Applied Sciences*, 2:2183.https://doi.org/10.1007/s42452-020-03573-6.

Olafisoye, E.R., Sunmonu, L.A., et al. (2013). Groundwater Contaminants' Investigation at Aarada Waste Disposal Site Using Geophysical and Hydro-Physicochemical Approach. *Journal of Environmental Science*, Toxicology And Food Technology, 2(4): Pp. 01-10.

Olayinka, A.I., & Olayiwola, M.A. (2001)."Integrated Use of Geoelectical Imaging and Hydrochemical Methods in Delineating Limits of Polluted Surface and Groundwater at a Landfill Site in Ibadan Area, South West Nigeria".

Omosanya, K.O., Akinmosin, A., & Balogun, J. (2014). A review of stratigraphic surfaces generated from multiple electrical sound ing and profiling. *RMZ Mater Geoenviron* 61(1):49–63

Oomkens, E., 1974. Lithofacies relations in the Late Quaternary Niger Delta Complex. Sedimentol., *Conference & exposition on Petroleum Geophysics*, 21: 195-222.

Palacky, G.J. (1988). Resistivity characteristics of geologic targets. In: Nabighian MN (ed) Investigations in geophysics, vol 3: electro magnetic methods in applied geophysics-theory, vol 1. *Society of Exploration Geophysicists, Tulsa*, pp 53–129

Parvin, F., & Tareq, S. M. (2021). Impact of landfill leachate contamination on surface and groundwater of Bangladesh: a systematic review and possible public health risks assessment. *Applied Water Science*, *11*(6), 100. *https://doi.org/10.1007/s13201-021-01431-3*

Ronald, I. (1988). "The Renaissance of Political Culture," American Political Science Review, *Cambridge University Press*, vol. 82(4), pages 1203-1230

Vander, Velpen, B.P.A (2004). "WIN RESIST™" Version 1.0 Resistivoty Depth Sounding Interpretation Software. M.Sc Research Project, ITC, Delf Netherland

Vander Velpen, B.P.A. (1988). RESIST version 1.0 M.Sc. Research Project ITC, Deft, Netherlands

**Copyright © 2026 The Author(s). This is an open-access article published by Khazar Journal of Water and Environment under the terms of the Creative Commons Attribution License which permits unrestricted use, distribution, and reproduction in any medium or format, provided the original work is properly cited.**